

Experimental Analysis of CSC-type Shear Connectors Behavior under Direct Shear: Pry-Out Test (I)

The use of steel and concrete composite sections has been recorded since the early 1950s, mainly in Europe and North America, as pioneers in the industrial production of steel elements. These systems have become popular in the world due to the efficiency of structural behavior, where steel withstands tension and concrete develops its bearing capacity in compression, being essential for the installation of stress transfer elements at the interface, called shear connectors. Recently, the use of cold-formed steel sections (CFS) has been included as a cost-effective alternative in the construction of small and medium-sized buildings. In this way, it complements concrete elements, allowing the formation of highly efficient systems, mainly in flooring systems. In this research the experimental validation of the behavior of CSC-type shear connectors is proposed, configured by Hurtado & Molina (2020), which are applicable to these CFS-concrete configurations. Pry-out tests were carried out, initially proposed by Anderson & Meinheit (2005), where the axial tensile load is applied to the steel section. This alternative experimental proposal differs from traditional push-out tests, since compressive loads can generate local buckling in steel shapes, particularly in CFS sections. The experimental results were statistically analyzed, evaluating the incidence of the compressive strength of the concrete, the thickness of the steel profile, and the spacing between connectors on the bearing capacity of the composite system. As a result of the research, the design formulation for CSC-type shear connectors in CFS-concrete composite sections is proposed.

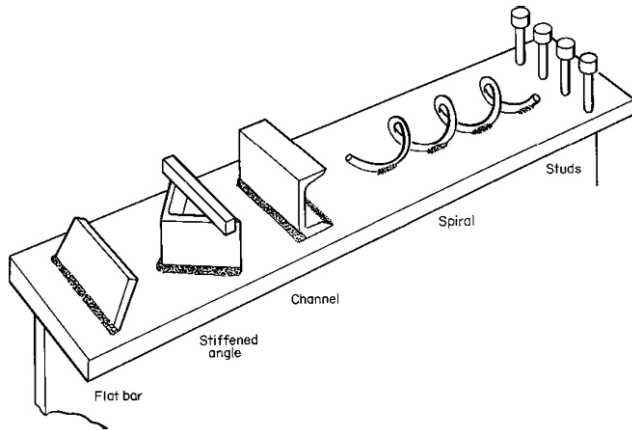
Keywords: Composite sections, CSC-type shear connector, Cold-formed steel (CFS), Design formulation.

Introduction

Since the late 1950s, composite sections have been used in building construction, with the Swiss pioneering in Europe with the construction of the Nestlé building in Vevey in 1959 (Crisinel, 1990). Subsequently, this system became widely known because of the advantages provided by the combination of materials, such as improved mechanical properties and efficiency. Thus, these composite systems became popular both in Europe and in the United States, the leading industrial powers of steel production.

Studs were the first elements used to transfer stresses between materials, ensuring connection and support. At that time, these elements had constructive advantages for their installation and manufacture. Over the years, the research on different types of shear connectors was expanded, with different proposals such as channel shapes, angle shapes, Perfobond rib plates, screw-type connectors, hooks, among others. These devices have different geometric and mechanical characteristics to transfer forces in composite systems in the most efficient way.

Figure 1. Types of Shear Connectors in Composite Sections



Source: Taken from Majdi et al. 2014

Due to the technical requirements of welding and the limitations of its use in unfavorable climatic conditions, the connector fastening system is also a relevant factor in the efficiency of the construction process (Crisinel, 1990). Similarly, welding has technical limitations to be applied efficiently in thin-walled elements (Figure 2).

Figure 2. Damages in CFS Steel Plates caused by Welding Process



Source: Erazo & Molina (2017).

Currently, the shear connectors approved in various international design codes are studs, channel shapes, Perfobond rib plates, and screw-type connectors. However, it is mandatory to carry out an experimental plan to validate the bearing resistance of any other type of unregulated device. Among the experimental tests proposed for the validation of the system capacity are the direct shear tests, called *push-out test*, and the long-scale beam test. Shear tests are easier to perform than bending tests due to the size of the specimens and their maneuverability, and provide more conservative results (Crisinel, 1990).

In this study, the alternative experimental pry-out test, originally designed by Anderson & Menheit (2005), is proposed. In this test, the load is applied by traction in the steel shape instead of compression, thus eliminating the possible local buckling problems generated mainly in thin-walled steel sections. In addition, this experimental arrangement is a cheaper alternative due to the geometric configuration.

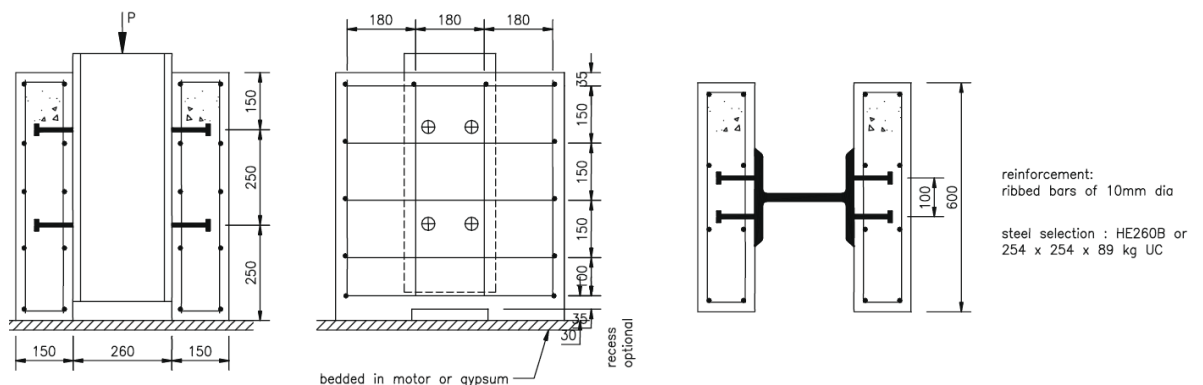
In the experimental configurations tested, the capacity of CSC-type shear connectors was validated. These devices were proposed by Hurtado and Molina (2020). The incidence of the concrete strength, the thickness of the steel shapes, and the spacing of the connectors were involved in the final capacity of the composite system. As a result of the research, the load-displacement curves of the system were obtained. The statistical incidence of the mentioned variables and their relevance in a design formulation for CSC-type shear connectors involved in CFS-concrete composite sections were evaluated.

Background

Traditionally, experimental tests to study the behavior and maximum capacity of shear connectors in composite systems are full-scale beam tests and push-out shear tests, which are protocolized in Eurocode 4 and are the most commonly used methodology to obtain design formulations.

Due to the specimen dimensions of each type of test, and the complexity of the setup, the push-out test is considered the easiest to perform. The specimens are made up of two concrete slabs attached to a steel section. The axial compressive load is applied monotonically on the steel element and the stresses are transferred to the slab through the shear connectors, as shown in Figure 3.

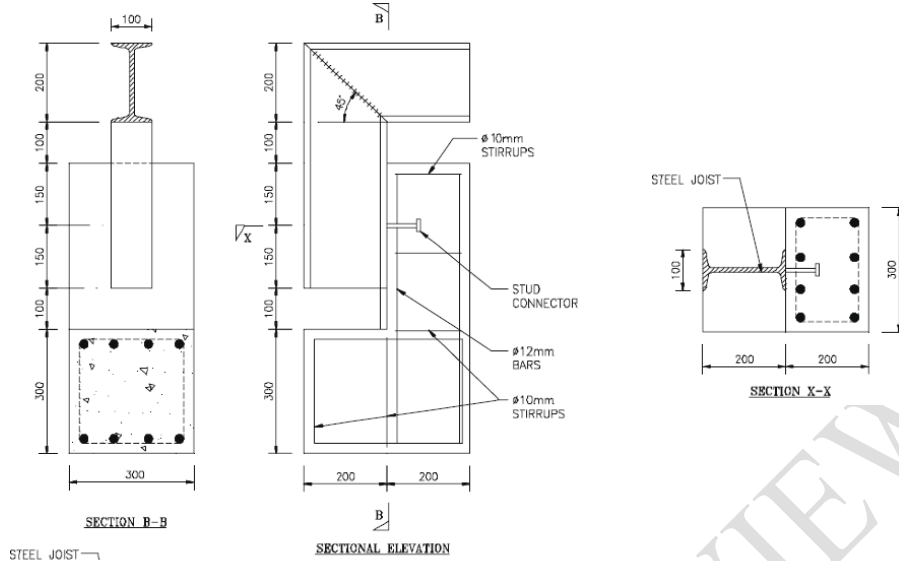
Figure 3. Push-out Test Setup



Source: Eurocode4

Likewise, the Indian code for the design of composite sections (IS 11384-1985) proposes a different experimental setup for shear testing. The interaction is induced by two L-sections of steel and concrete joined by shear connectors at the interface. This arrangement allows loads to be applied over larger areas and specimens to be supported, as shown in the scheme presented in Figure 4.

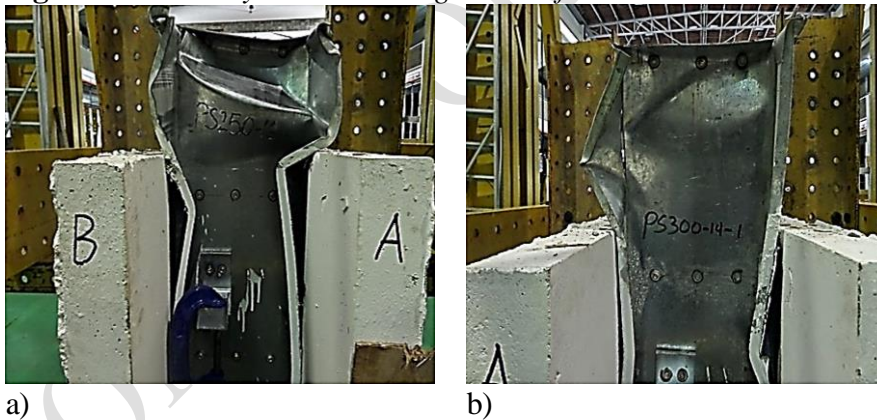
1 **Figure 4.** Setup of Shear Test proposed in the Indian Design Code



2 Source: IS 11384-1985

3
4 According to the experimental test conditions, mainly in cold-formed steel
5 sections, compressive loads have shown the induction of premature failure by
6 local buckling in the steel plates without effectively validating the connector
7 capacity, as presented in Lawan's (2016) research and shown in Figure 5.

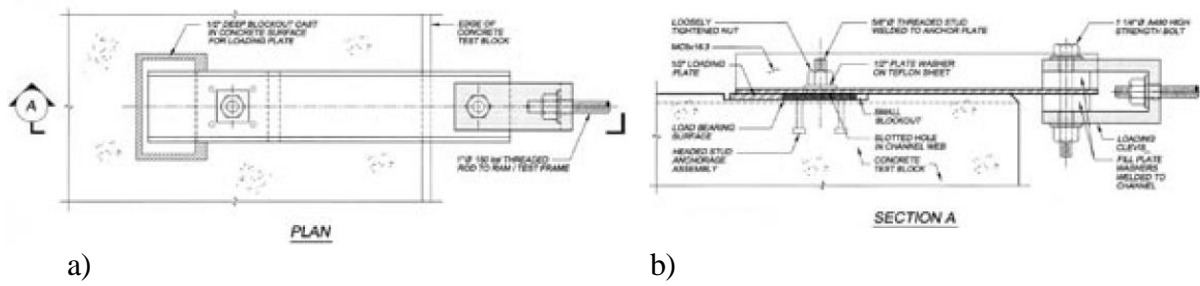
8
9 **Figure 5.** Failure by Local Buckling in Cold-formed Steel Sections in Push-out Test



10 Source: Lawan et al. 2016.

11
12 Anderson & Menheit (2005) alternatively proposed the pry-out shear test,
13 which eliminates this logistical disadvantage. The configuration of the specimens
14 is modified from the *push-out tests* to a single concrete slab. The monotonic load
15 is applied as traction on the steel profile, as shown in Figure 6.

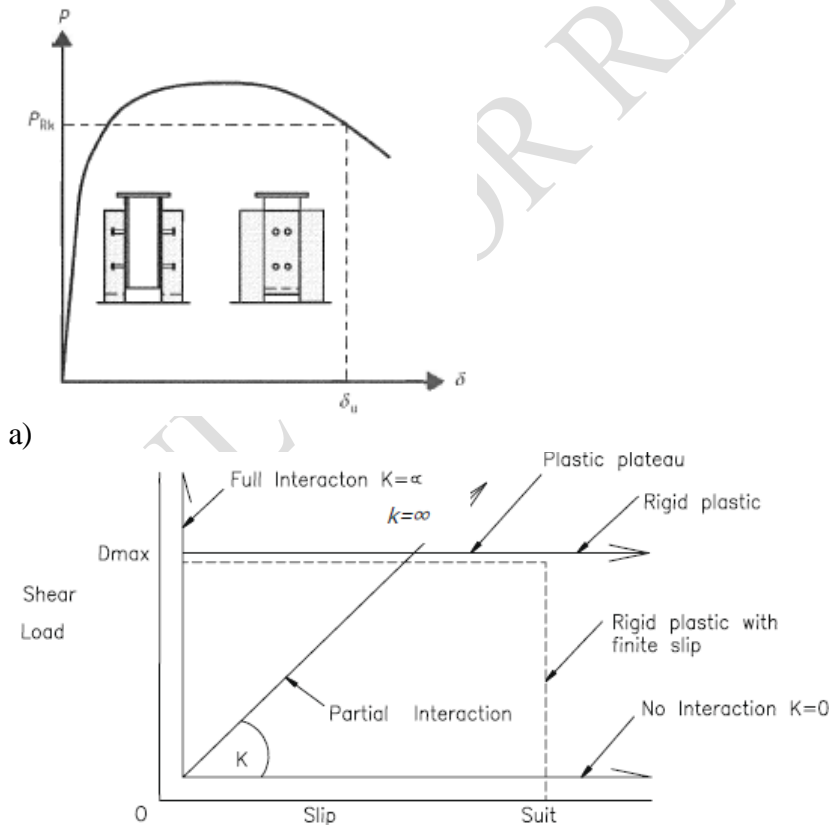
1 **Figure 6. Setup of Alternative Pry-out Test**



2 Source: Anderson & Menheit., 2005.

3
4 Load vs. displacement curves are obtained as a result of the characterization
5 of the behavior and capacity of the shear connectors in experimental tests. These
6 curves make it possible to compare the performance of different configurations of
7 the composite systems with different study parameters, such as the type of
8 connector, the strength of the concrete, the spacing between connectors, the
9 strength of the steel, among others. (Figure 7).

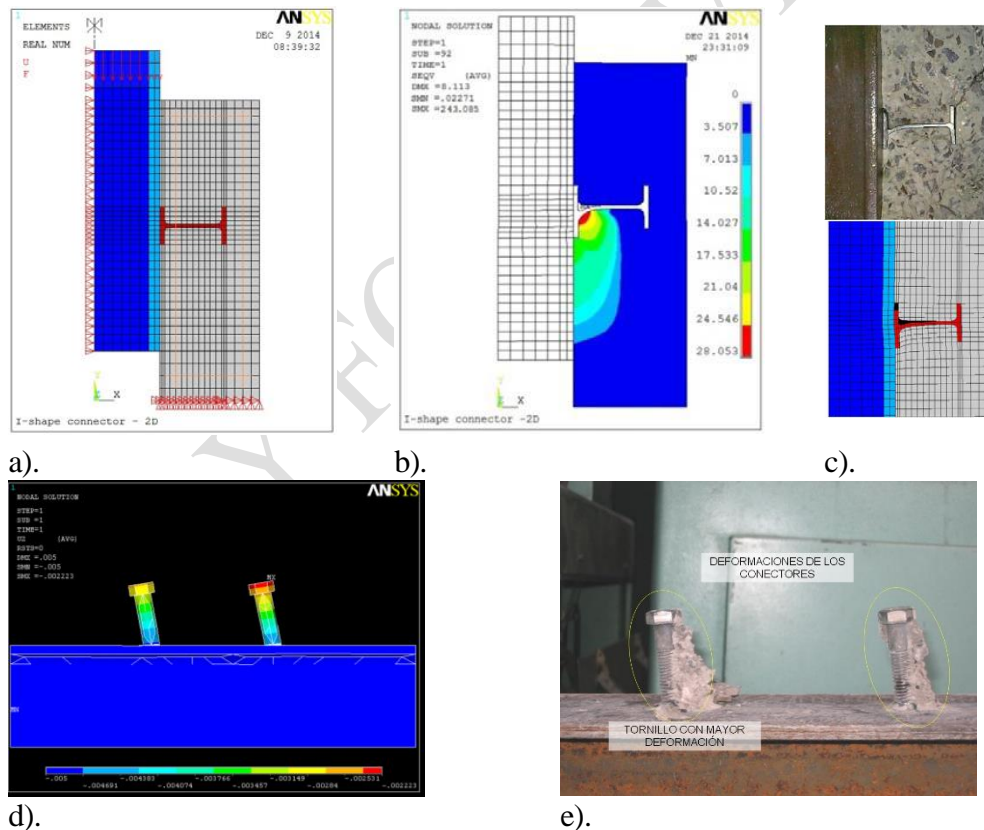
11 **Figure 7. Load vs. Displacement Curve. a). Typical Scheme of Behavior. b)**
12 **Idealization of Analytical Behavior**



13 Source: a). Eurocode4. b). Johnson & Buckby. 1994.

Along with experimentation, numerical simulation has become a very powerful analytical tool to achieve a good representation of computational mechanics systems, applying the finite element method (FEM), as reported by Crisinel (1990), Jeong et al. (2005), Hurtado (2007), Derlatka et al. (2019), Titoum et al. (2016), among others (Figure 8). Calibration in numerical models from material properties and constitutive models of materials, configuration of an adequate geometry, and correct simulation of support conditions are the most important factors to achieve a good representation of analytical models using specialized software. In addition, numerical models allow access to analysis results anywhere in the model.

Figure 8. Two-dimensional computational model of push-out test. a). I-type connector modeling geometry. b). I-type connector analysis result. c). Comparison of connector deformations in experimental test and I-type connector simulation. d). Final state of displacements screw-type shear connector in three-dimensional numerical model. e). Final state of displacements screw shear connector in experimental specimen



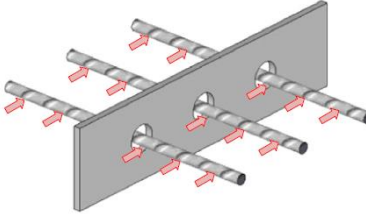
Source: a), b) and c) from Titoum et al. 2016. d) and e) from Hurtado 2007.

Through this methodology of direct shear tests, both experimental and through analysis of numerical simulation models, it has been possible to statistically correlate different parameters that directly affect the capacity of composite systems. In this way, different design expressions have been proposed

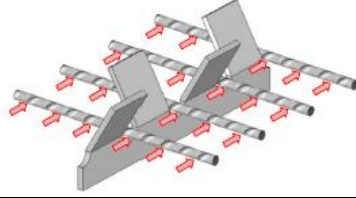
to estimate the capacity of the shear connectors, without being standardized in any international design code.

Table 1 lists different design formulations for estimating the bearing capacity of different types of shear connectors that have been reported in different investigations, but have not been included in any design code for the configuration of composite sections.

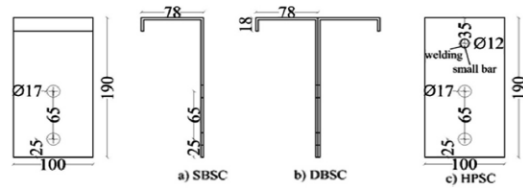
Table 1. Design Formulations for Different Types of Shear Connectors, registered in Investigations

Author	Design formulation
Perfobond rib connectors	
	
Oguejiofor & Hosain (1994)	$Q_{rib} = 0.59A_{cc}\sqrt{f'_c} + 1.23A_{tr}F_y + 2.87n_{rib}\pi d_{rib}^2\sqrt{f'_c}$ (1)
Oguejiofor & Hosain (1997)	$Q_{rib} = 4.50h_{rib}t_{rib}f'_c + 0.91A_{tr}F_y + 3.31n_{rib}\pi d_{rib}^2\sqrt{f'_c}$ (2)
Hosaka et al. (2000)	$Q_{hole} = 3.38 \sqrt{\frac{t_{rib}}{d_{rib}}} d_{rib}^2 f'_c - 39 \times 10^3$ $22 \times 10^3 < \sqrt{\frac{t_{rib}}{d_{rib}}} d_{rib}^2 f'_c < 194 \times 10^3$ (3)
Hosaka et al. (2000)	$Q_{hole} = 1.45[(d_{rib}^2 - d_{tr}^2)f'_c + d_{tr}^2 F_u] - 26.1 \times 10^3$ $51 \times 10^3 < (d_{rib}^2 - d_{tr}^2)f'_c + d_{tr}^2 F_u < 488 \times 10^3$ (4)
Sara & Bahram (2002)	$Q_{rib} = 0.747b_{ecs}h_{ecs}\sqrt{f'_c} + 0.413b_f L_c + 1.66n_{rib}\pi \left(\frac{d_{rib}}{2}\right)^2 \sqrt{f'_c} + 0.91A_{tr}F_y$ (5)
Medberry & Shahrooz (2002)	$Q_{slab} = 0.90A_{tr}F_y + 0.747b_{ecs}h_{ecs}\sqrt{f'_c} + 0.413b_f L_c + 1.304n_{rib}d_{rib}^2\sqrt{f'_c}$ (6)
Verissimo et al. (2007)	$Q_{rib} = 0.404 \frac{h_{rib}}{b_{rib}} h_{rib} t_{rib} f'_c + 2.37n_{rib}d_{rib}^2\sqrt{f'_c} + 0.16A_{cc}\sqrt{f'_c} + 31.85 \times 10^6 \left(\frac{A_{tr}}{A_{cc}}\right)$ (7)
Al-Darzi et al. (2007)	$Q_{rib} = 0.762h_{rib}t_{rib}f'_c - 7.59 \times 10^{-4}A_{tr}F_y + 3.97n_{rib}d_{rib}^2f'_c + 255310$ (8)
Ahn et al. (2010) 1 connector	$Q_{rib} = 3.14h_{rib}t_{rib}f'_c + 1.21A_{tr}F_y + 3.79n_{rib}\pi \left(\frac{d_{rib}}{2}\right)^2 \sqrt{f'_c}$ (9)
Ahn et al. (2010) 2 connectors	$Q_{rib} = 2.76h_{rib}t_{rib}f'_c + 1.06A_{tr}F_y + 3.32n_{rib}\pi \left(\frac{d_{rib}}{2}\right)^2 \sqrt{f'_c}$ (10)
Zhao & Liu.	$Q_{hole} = 1.38(d_{rib}^2 - d_{tr}^2)f'_c + 1.24d_{tr}^2F_y$ (11)

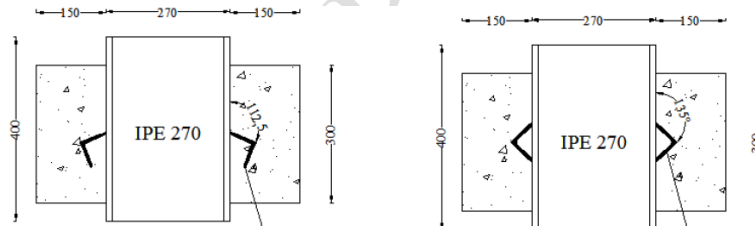
(2012)		
Liu et al. (2016)	$Q_{hole} = 1.85[(A_{rib} - A_{tr})f'_c + A_{tr}F_u] - 26.1 \times 10^3$	(12)
Liu et al. (2016)	$Q_{hole} = 1.76(A_{rib} - A_{tr})f'_c + 1.58A_{tr}F_y$	(13)
Y-Type perfobond rib connector		



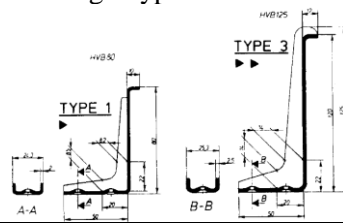
Jung et al. (2013)	$Q_{Y.rib} = 3.428 \left(\frac{d_{rib}}{2} + 2h_{rib} \right) t_{rib} f'_c + 1.213 A_{tr} F_y + 1.9 n_{rib} \pi \left(\frac{d_{rib}}{2} \right)^2 \sqrt{f'_c} + 0.438 m_{rib} h_{rib} s_{rib} \sqrt{f'_c}$	(14)
Bolted CFS shear connector		



Tahir et al. (2019)	$Q_{con} = 4.50 h_{con} t_{con} f'_c$	(15)
Angle-type shear connectors		



Shariati et al. (2017) Angle 112.5°	$Q_{112.5} = 1.57 \sqrt{f'_c} t_{con}^{0.35} L_{con}^{0.48}$	(16)
Shariati et al. (2017) Angle 135°	$Q_{135} = 11 \sqrt{f'_c} h_{con}^{0.48} L_{con}^{-0.25}$	(17)
Bolted angle-type shear connectors		



Crisinel (1990)	$Q_{con} = 0.45 \sqrt{f'_c A_c} \leq 0.50 A_c \sqrt{f'_c E_c}$	(18)
-----------------	--	------

Source: Authors.

1
2
3

Materials and Methods

Material Characterization

The properties of the materials were taken from their nominal values for steel elements (Table 2) and experimental validation for concrete cylinders. In this case, 3 different concrete compressive strengths were used: 14.8MPa, 22.9MPa, and 33.5MPa (Table 3).

The nominal properties of the steel elements are shown in Table 2.

Table 2. Nominal Properties of the Steel Components in Experimental Specimens

	CSC-Type shear connectors (ASTM A424 - Type II) [MPa]	Self-drilling screws (SAE 1022) [MPa]	Steel reinforcement (ASTM A706) [MPa]	Steel section (ASTM A1011) [MPa]
Modulus of elasticity (Es)	200.000	200.000	200.000	200.000
Yield strength (fy)	240	205	420	350
Ultimate tensile strength (fu)	350	380	560	420

Source: Authors.

Experimental Test

In this study, experimental specimens were configured with CSC-type shear connectors and reinforcing bars. The devices were embedded in a 450mmx300mmx100mm concrete slab (Figure 9). In the structural configuration, N°10 self-drilling screws (4.83mm in diameter) were used for all configurations. Structural C220x80, 600mm in length, was used as steel element in various thicknesses (Table 3).

Figure 9. Elaboration process of the specimens for the pry-out test. a) Installation of shear connectors. b) Concrete pouring. c) Assembly of the entire system



a)



b)

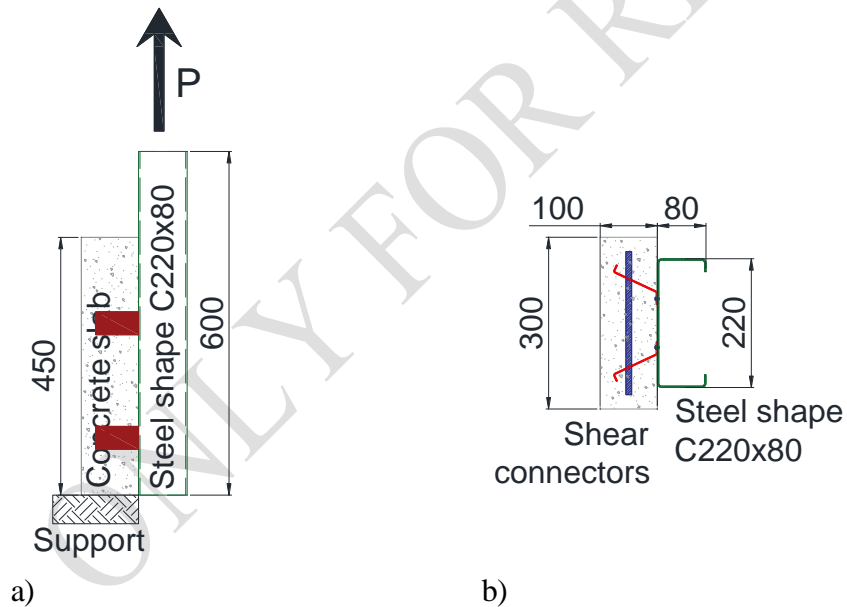


c)

Source: Authors.

The load on the system was applied monotonically as an axial traction on the steel profile; a hydraulic jack was used to apply the load. The concrete slab was fixed to the base of the Universal machine by means of a rigid system, to ensure the transfer of stresses through the shear connectors, as shown in Figure 10. The load was increased made by control of displacement.

Figure 10. Pry-out Test Setup. a) Scheme of Load Application. b) Cross-section. (Units in mm). c) Assembly of the Experimental Test



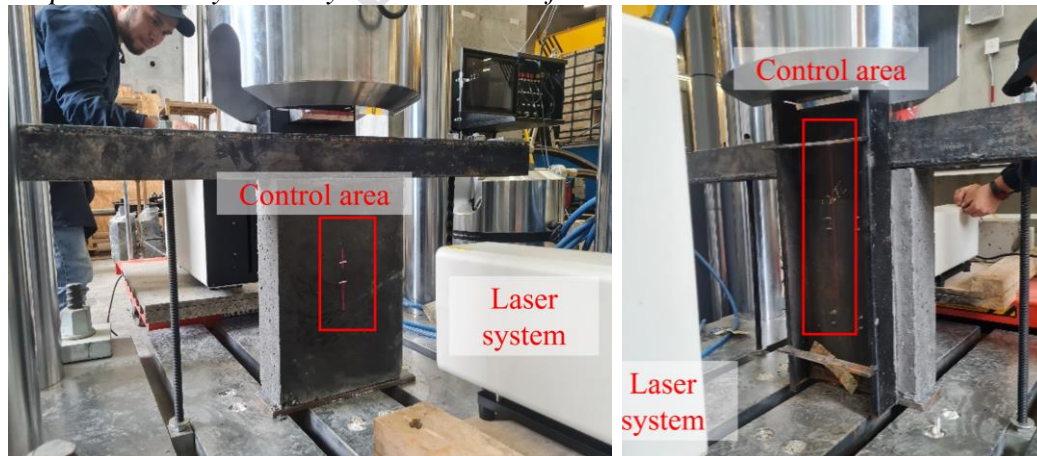


c)

Source: Authors.

Load and displacement data were recorded directly by the equipment's data acquisition system. In addition, laser measurement systems were installed to verify any differential movement between the concrete slab and the steel element. The instrumentation is shown in Figure 11.

Figure 11. *Experimental Test Instrumentation in the Pry-out Test. a) Measurement of Displacements by Laser System in the Concrete Plate. b) Measurement of Displacements by Laser System in Steel Profile*



a)

Source: Authors.

b)

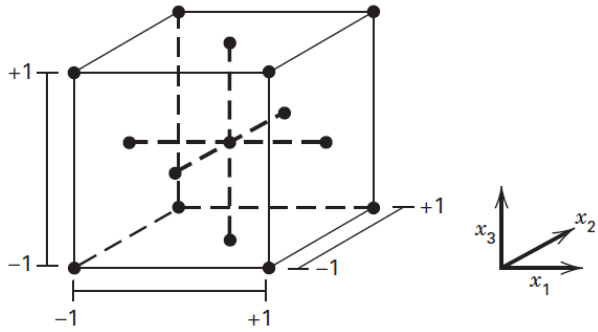
Finally, the condition of maximum displacements of the system as well as the ultimate loads and failure modes were verified. The configuration of the specimens is defined in Table 3.

Experiment Design

The Central Composite Face-Centered (CFC) design was chosen to evaluate the contribution of the study variables to the system behavior, allowing second-order fittings. In this case, the compressive strength of the concrete, the thickness of the steel profile, and the spacing between the connectors were defined as the main study parameters.

Based on the methodology, Table 3 lists the specific design points from the entire experimental matrix that were selected for testing. Figure 12 shows the graphical selection of design points. Values +1 and -1 indicate coded variables between the maximum and minimum values in the natural variables (x_1 , x_2 and x_3), respectively, labeled as (A), (B) and (C)

Figure 12. Central Composite Face-centered design: Identification of design points



Source: Montgomery, 2013

Results and Discussion

The compressed data report from the experimental tests is shown in Table 3 and the load-displacement curves are shown in Figure 13.

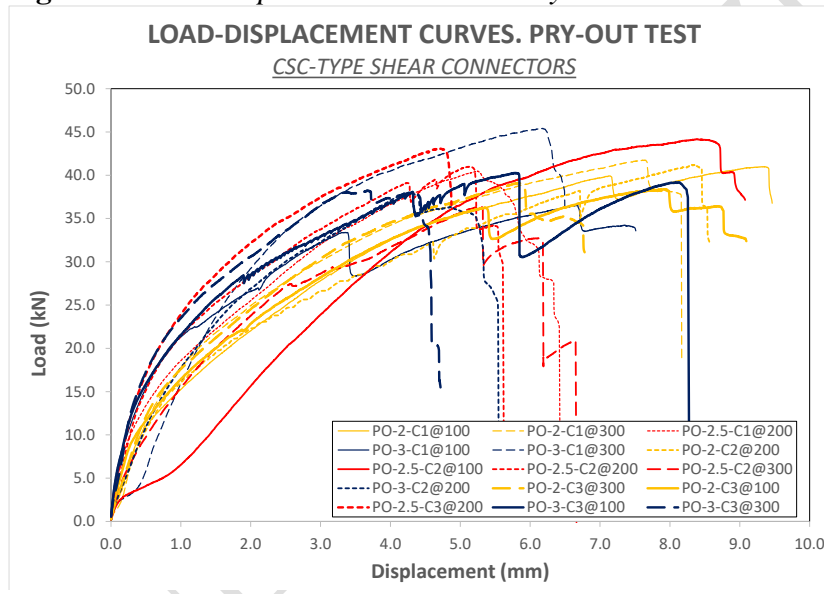
Table 3. Record of Data from Pry-out Tests

N°	Specimen	Compressive strength of concrete (A)	Thickness of steel section (B)	Spacing between connectors (C)	Maximum force of reaction	Maximum displacement	Failure mode
		[MPa]	[mm]	[mm]	[N]	[mm]	
1	PO-2-C1@100	14.8	2.0	100	20413.99	9.07	Shear in screws
2	PO-2-C1@300	14.8	2.0	300	20880.09	7.64	Shear in screws
3	PO-2.5-C1@200	14.8	2.5	200	20241.20	5.25	Shear in screws
4	PO-3-C1@100	14.8	3.0	100	18249.52	6.65	Shear in screws

5	PO-3-C1@300	14.8	3.0	300	22705.08	6.16	Shear in screws
6	PO-2-C2@200	22.9	2.0	200	20600.25	8.34	Shear in screws
7	PO-2.5-C2@100	22.9	2.5	100	22082.57	8.39	Shear in screws
8	PO-2.5-C2@200	22.9	2.5	200	20500.16	5.13	Shear in screws
9	PO-2.5-C2@300	22.9	2.5	300	18193.47	5.28	Shear in screws
10	PO-3-C2@200	22.9	3.0	200	19023.60	4.30	Shear in screws
11	PO-2-C3@100	33.5	2.0	100	19195.98	7.93	Shear in screws
12	PO-2-C3@300	33.5	2.0	300	19563.39	5.82	Shear in screws
13	PO-2.5-C3@200	33.5	2.5	200	21536.84	4.72	Shear in screws
14	PO-3-C3@100	33.5	3.0	100	20134.27	5.79	Shear in screws
15	PO-3-C3@300	33.5	3.0	300	19110.85	3.69	Shear in screws
16	PO-2.5-C2@200	22.9	2.5	200	20500.16	5.13	Shear in screws

Source: Authors.

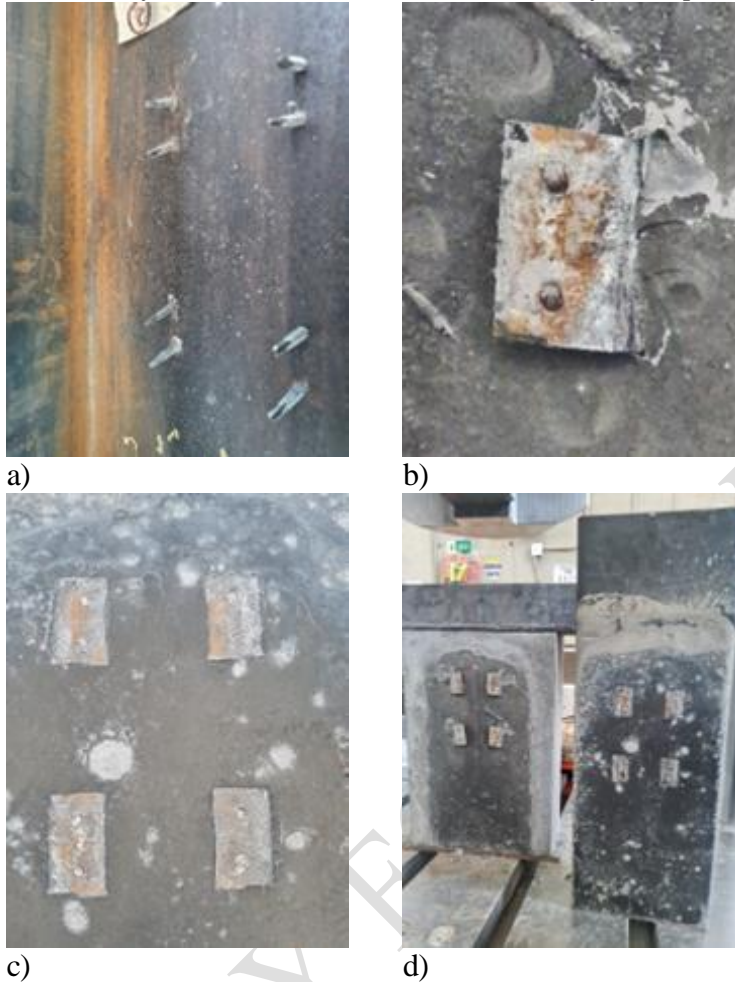
Figure 13. Load-displacement Curves in Pry-out Test



Source: Authors

According to the results, the failure mechanism starts with the inclination of the fastening screws in the connectors. This process started earlier in the thinner steel section (Figure 14 a)). Subsequently, with relative displacements greater than 4mm and reaching up to 9mm, and depending on the configuration, short cracks were observed in the connectors as well as failure by shear in the screws in all the specimens (Figure 14 b)), with all configurations of the composite system decoupling (Figure 14 d)).

1 **Figure 14.** *Failure mechanism of the composite system. Tilted screws after the*
 2 *loading process and shear failure. b). Tear detail in shear connectors. c). Final*
 3 *condition of CFS sections. (d) Final condition of uncoupled specimens*

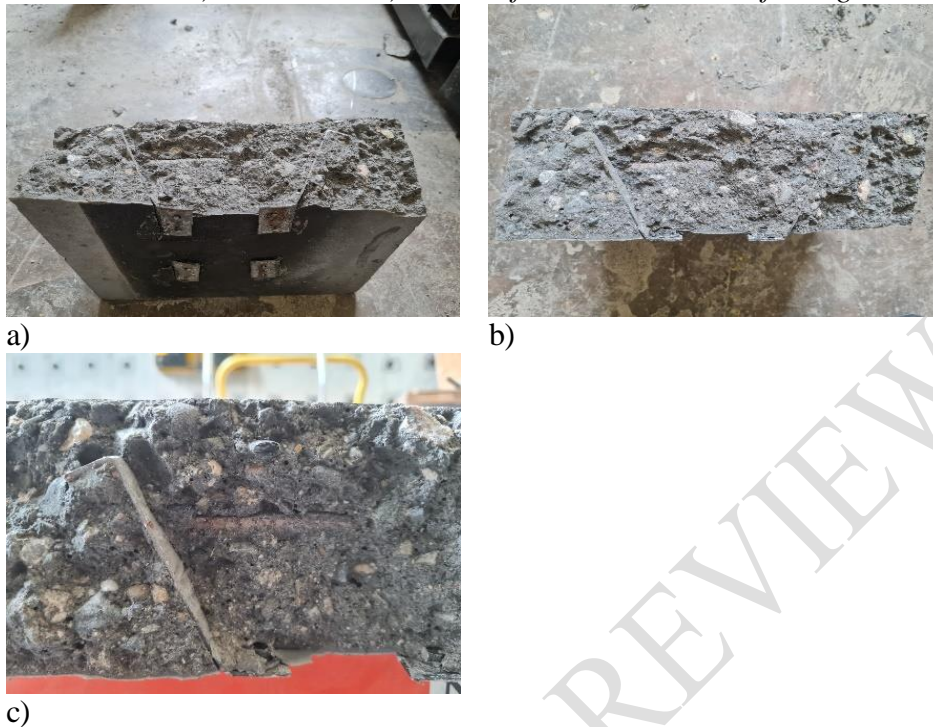


Source: Authors

This failure condition, under service conditions in a flooring system, would imply a change in structural behavior to a non-composite system of slab and beams that must be able to withstand gravity loads.

Figure 15 shows the state of the connectors on the concrete slab, allowing their integrity within the concrete matrix to be perceived. The geometric arrangement allowed the concrete to flow under the connector and around the reinforcement while remaining completely confined. In this way, the full bearing capacity was effectively transferred across all system components.

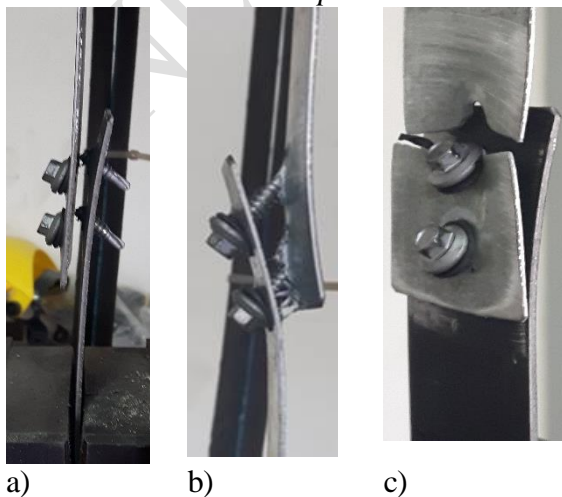
1 **Figure 15.** *Final state of the shear connectors embedded in the concrete slab. a).*
 2 *General view. b). Front view. c). Detail of connector and reinforcing bar*



Source: Authors

These results confirm the experimental behavior proposed by Hurtado & Molina (2020), where structural elements with thicknesses greater than 2mm presented a failure mechanism by shear in screws. At lower thicknesses, the predominant failure mode was induced by tearing of the steel plates, as shown in Figure 16.

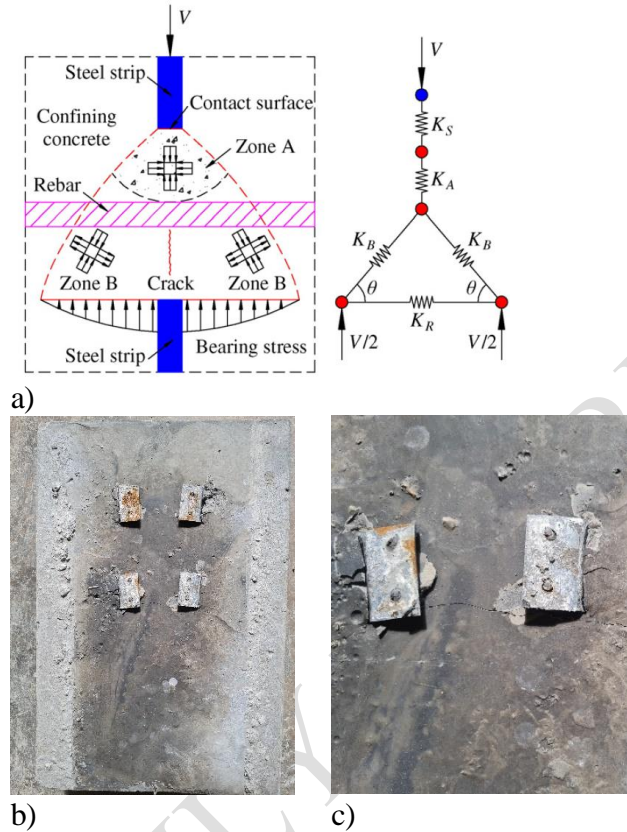
Figure 16. *Failure modes presented in the screw shear test. a) Failure due to screw shear. b) Failure due to screw tilting and plate separation. c) Failure due to tension on the net section in plate*



Source: Authors

As shown in Figure 17, additional transverse cracks were likely in specimens with lower compressive strength concrete. This confirms the effectiveness of the geometric and mechanical configuration of the connector. Thus, the inclusion of the reinforcing bar guarantees the dispersion of the cracks induced by the axial load.

Figure 17. Shear transfer mechanism including reinforcing bar. a) Theoretical idealization of the mechanism. b) General view induction of transverse cracks in concrete plate. c). Detail induction of transverse cracks in concrete plate



Source: a). Taken from Liu et al. 2015. b). and c). Authors

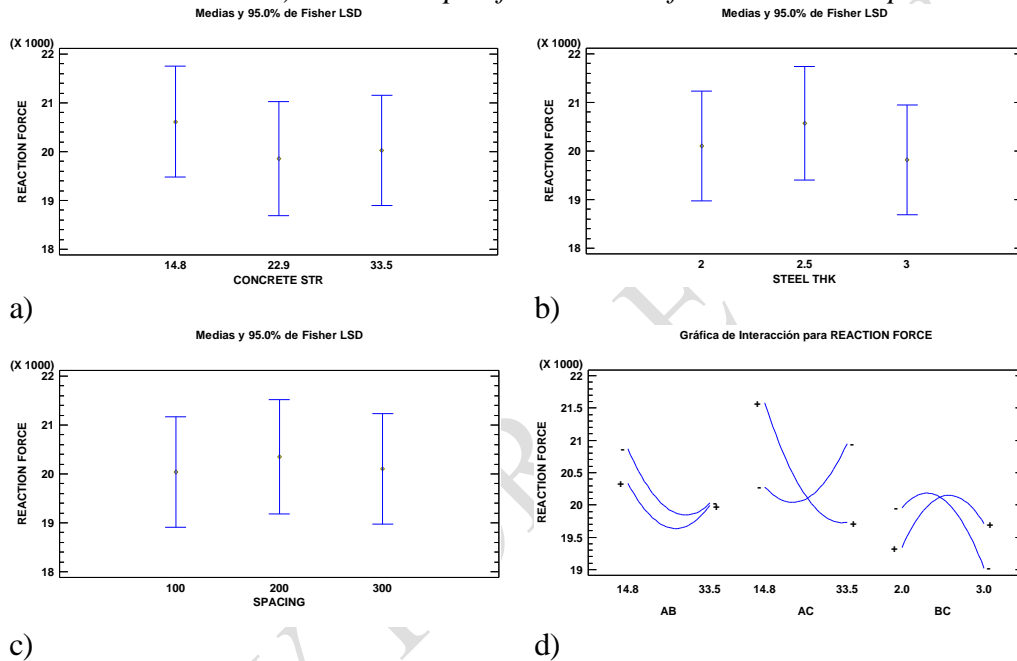
This failure condition aims to predict that, under the same conditions of this research, the compressive strength of the concrete is not relevant in the maximum capacity of the composite system, where the failure is governed by shear in screws.

Statistical Response

The statistical response is approached from the behavior of the maximum reaction force of the system and the maximum displacement reached, evaluating the incidence of the variables involved in the study on the performance and maximum capacity of the system: (A) compressive strength of concrete, (B) thickness of the steel profile and (C) spacing between connectors (Table 3).

Shear in self-drilling screws was the failure mode that determined the damage in all specimens. Therefore, there were no statistically significant differences among the experimental arrangements tested. Figure 18 shows the statistical confidence intervals for the maximum load reaction with a 95% probability of failure for both the concrete compressive strength (Figure 18 a)), the steel shape thickness (Figure 18 b)), and the spacing between connectors (Figure 18 c)), where the overlapping response values show statistical equality.

Figure 18. Confidence interval for maximum load reaction with 95% probability. a) Compressive strength of concrete. b) Thickness of the steel shape. c) Spacing between connectors. d) Interaction plot for maximum force reaction response

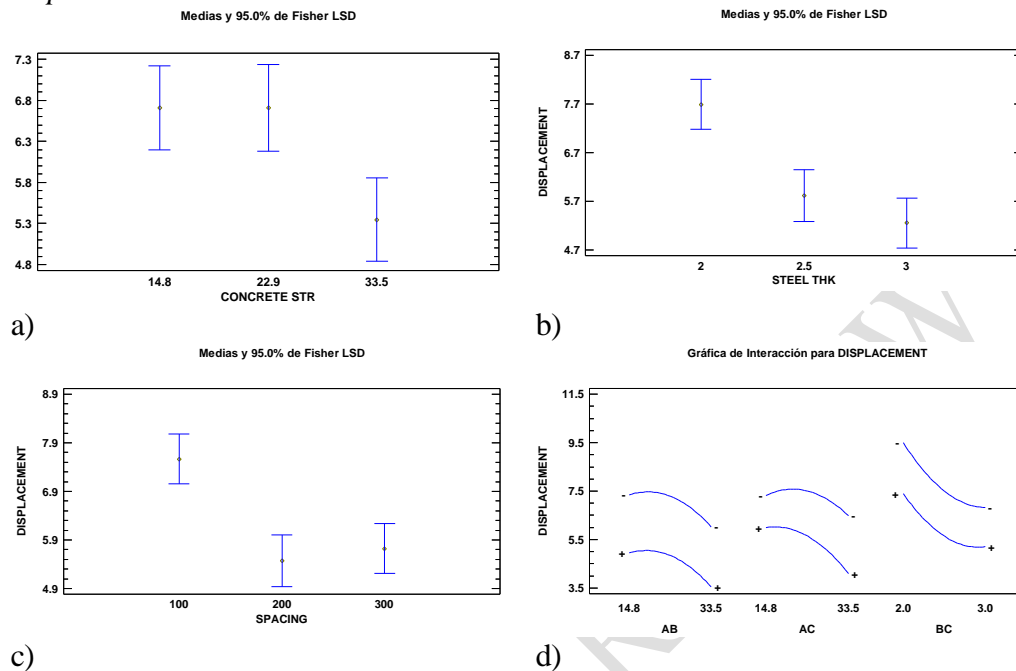


Source: Authors

Figure 18 d) shows the interaction plot for all the parameters, where the intersection implies the simultaneous work of all the variables under the proposed configurations.

On the other hand, to evaluate the maximum displacements, the confidence intervals of the statistical response allow to appreciate significant differences for all the variables studied. It has been concluded that the failure condition presents sensitive deformations depending on the different arrangements of the composite systems, with values exceeding 6mm. (Figure 19).

Figure 19. Confidence interval for displacement load reaction with 95% probability. a) Compressive strength of concrete. (b) Thickness of the steel shape. c) Spacing between connectors. d) Interaction plot for maximum force reaction response



Source: Authors

Unlike the maximum reaction response, the displacement condition does not show the interaction of the variables, which indicates that changing the values of each one of them separately affects the final displacement condition. (Figure 19 d).).

Parametric Analysis

The parametric analysis made it possible to determine the incidence of the studied variables in the final states of behavior of the composite systems, in particular the maximum reaction loads and the maximum displacements.

Effect of the Compressive Strength of the Concrete

In some specimens, cracks appeared in the concrete slabs as part of the simultaneous failure mechanism of the composite system without total failure of the concrete. As shown in Figure 18 a) and Figure 19 a), this variable is not considered statistically significant in the maximum load capacity of the composite systems, but it does make a difference in the maximum displacement condition. The lower strengths show larger displacements according to the stiffness of the materials.

Effect of Steel Profile Thickness

Similarly to concrete, the thickness of the steel section only affects the stiffness condition of the system, implying greater displacements in elements with lower thicknesses, as can be seen in Figure 18 b) and Figure 19 b). The steel profiles did not show any local or global damage in any of the configurations tested.

Effect of Connector Spacing

The spacing between connectors marked a strong difference in the maximum relative displacements between the materials, which were greater in the specimens with smaller spacing (Figure 19 c)). This situation indicates that smaller separations give the system greater ductility before failure. There is no statistically significant difference regarding the maximum loads (Figure 18 c)).

Design Formulation

According to the behavior of the studied composite systems, the design expression of CSC-type shear connectors (19) is proposed for failures in the fastening system due to shear in the screws without major effect on the other components of the system:

$$Q_n = 13000 \cdot \alpha \cdot f_c^{0.20} \cdot t_{st}^{0.20} \leq 4 \cdot A_{sc} \cdot F_u \quad (1)$$

The first part of the equation is related to concrete fracture failure, adjusted from the simulation results of Hurtado and Molina (2021). α is an experimental validation parameter, taken as 1.0 for the graph in Figure 20.

Table 4 shows several cases of estimation of the maximum loads of the composite system based on the proposed design equation. It also includes the ratio of the maximum experimental load to the estimated load, with emphasis on the proposal for the No.10-screws that were tested. It can be seen that the experimental load is about 20% higher than the estimated load.

Table 4. *Estimated Failure Loads for Shear in Self-drilling Screws from the proposed Design Equation*

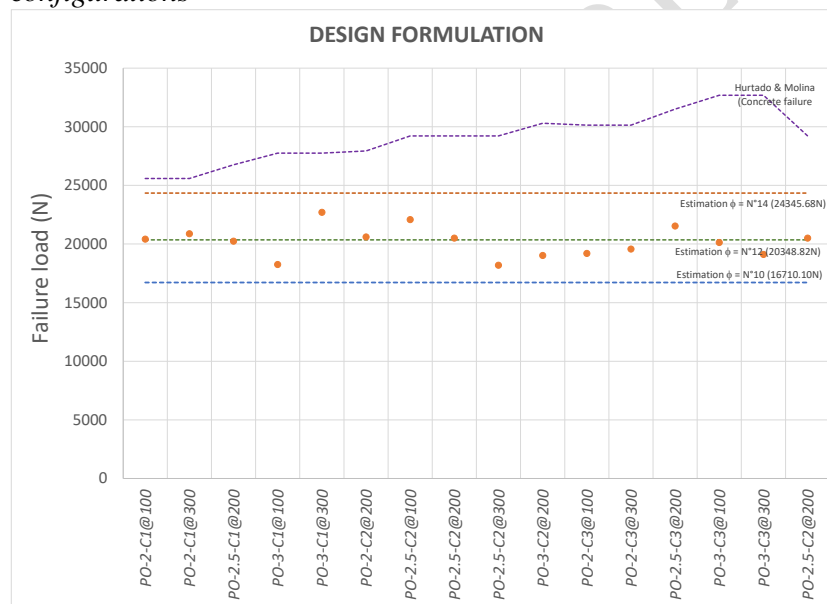
N°	Specimen	Maximum experimental reaction force	Nominal failure load for N°10-Screws	Nominal failure load for N°12- Screws	Nominal failure load for N°14- Screws
		[N]	[N]	[N]	[N]
1	PO-2-C1@100	20413.99	16710.10	1.22	20348.82 1.00 24345.68 0.84
2	PO-2-C1@300	20880.09	16710.10	1.25	20348.82 1.03 24345.68 0.86
3	PO-2.5-C1@200	20241.20	16710.10	1.21	20348.82 0.99 24345.68 0.83
4	PO-3-C1@100	18249.52	16710.10	1.09	20348.82 0.90 24345.68 0.75
5	PO-3-C1@300	22705.08	16710.10	1.36	20348.82 1.12 24345.68 0.93

6	PO-2-C2@200	20600.25	16710.10	1.23	20348.82	1.01	24345.68	0.85
7	PO-2.5-C2@100	22082.57	16710.10	1.32	20348.82	1.09	24345.68	0.91
8	PO-2.5-C2@200	20500.16	16710.10	1.23	20348.82	1.01	24345.68	0.84
9	PO-2.5-C2@300	18193.47	16710.10	1.09	20348.82	0.89	24345.68	0.75
10	PO-3-C2@200	19023.60	16710.10	1.14	20348.82	0.93	24345.68	0.78
11	PO-2-C3@100	19195.98	16710.10	1.15	20348.82	0.94	24345.68	0.79
12	PO-2-C3@300	19563.39	16710.10	1.17	20348.82	0.96	24345.68	0.80
13	PO-2.5-C3@200	21536.84	16710.10	1.29	20348.82	1.06	24345.68	0.88
14	PO-3-C3@100	20134.27	16710.10	1.20	20348.82	0.99	24345.68	0.83
15	PO-3-C3@300	19110.85	16710.10	1.14	20348.82	0.94	24345.68	0.78
16	PO-2.5-C2@200	20500.16	16710.10	1.23	20348.82	1.01	24345.68	0.84

Source: Authors

Similarly, Figure 20 shows the behavior of the experimental response versus the estimated capacities for various diameters of self-drilling screws used as a fastening system for CSC-type shear connectors.

Figure 20. Estimation loads based on design equation proposed for different configurations



Source: Authors

Conclusions

The pry-out test methodology for the evaluation of the capacity of composite systems has proven to be a reliable experimental alternative, particularly for cold-formed steel sections (CFS), where the effect of local buckling potential, which occurs in traditional push-out tests due to compressive load, is mitigated. This

alternative experimental test can even be extrapolated to composite section configurations using hot-rolled sections (HRS) with greater plate thicknesses.

The experimental validation of the CFS-Concrete composite system, using CSC-type shear connectors, under direct shear loads, allowed the evaluation of the working conditions of the system and its failure mechanism. This mechanism started as rotation in the self-drilling screws as fastening elements and a limited tear in the connector plate. In a similar way, specimens with lower resistances showed cracks in the concrete slab. Finally, in all the configurations tested, the screws were cut without affecting the steel profile, thus decoupling the composite system, but without loss of the integrity of the elements.

Although the experimental parameters validated in this research were not statistically different for the maximum reaction loads, it was possible to find differences in the ductility conditions of the system. This meant greater relative displacements with lower concrete resistances, lower steel profile thicknesses, and smaller spacings, reaching values greater than 6mm, as the limit of Eurocode4 for ductile shear connectors.

Finally, the design expression of CSC-type shear connectors is proposed, to be used in the design of CFS-concrete composite systems, where the failure is projected by shear in the self-drilling screws as the fastening mechanism.

References

- Ahn, J.H., Lee, C.G., Won, J.H. & Kim, S.H. Shear resistance of the perfobond-rib shear connector depending on concrete strength and rib arrangement. *Journal Constructional of Steel Research*, 66. (2010). 295-307.
- Al-Darzi, S.Y.K., Chen, A.R. & Liu, Y.Q. finite element simulation and parametric studies of perfobond rib connector. *American Journal of Applied Science*, 4 (3). (2007). 122-127.
- Anderson, N. & Meinheit, D. Design criteria for headed studs groups in shear. *PCI Journal*. (2000). 46-75.
- Anderson, N. & Meinheit, D. Pry-out capacity of cast-in headed studs anchors. *PCI Journal*. (2005). 90-112.
- Crisinel, M. Partial-interaction analysis of composite beams with profiled sheeting and non-welded shear. *Journal of Constructional Steel Research*, 15. (1990) 65-98.
- Derlatka, A., Lacki, P., Nawrot, J. & Winowiecka, J. Numerical and experimental test of steel concrete composite beam with the connector made of top-hat profile. *Composite Structures*, 211. (2019). 244-253.
- Erazo, L. & Molina, M. Comportamiento de conectores de cortante tipo tornillo en secciones compuestas con lámina colaborante (In Spanish). Thesis of master's degree. Universidad Nacional de Colombia. (2017).
- European Committee Standardization. Eurocode 4: Design of composite steel and concrete structures. (2004).
- Hosaka, T., Mitsuki, K., Hiragi, H., Ushijima, Y., Tachibana, Y. & Wantabe, H. An experimental study on shear characteristics of perfobond strip and its rational strength. *Journal of Structural Engineering JSCE* 46A. (2000). 1593-1604.
- Hurtado, X.F. & Molina, M. Alternative fastening mechanism for shear connectors with cold-formed steel shapes involved in composite sections. *Athens Journal of Technology and Engineering*, 7(2). (2020). 133-156.

- 1 Hurtado, X.F. & Molina, M. Behavior of CSC-type shear connectors under pry-out shear
2 test: analytical study. *Materials Science Forum* Vol. 1046. (2021). 45-58.
- 3 Hurtado, X. Comportamiento de conectores de cortante tipo tornillo de resistencia grado 2
4 (dos) para un sistema de sección compuesta con concreto de 21MPa ante sollicitación
5 de corte directo. (In Spanish). Thesis of master's degree. Universidad Nacional de
6 Colombia. (2007).
- 7 Hurtado, X. & Molina, M. Geometrical and mechanical optimization of shear connectors
8 for CFS-concrete composite systems. In *The 2020 Structures Congress*. (2020). 25-
9 28.
- 10 Indian Standards Institution. IS 11384-1985. Indian standard code of practice for
11 composite construction in structural steel and concrete. (1986).
- 12 Jeong, Y.J., Kim, H.Y. & Kim, S.H. partial-interaction analysis with push-out test. *Journal*
13 *of Constructional Steel Research* 61. (2005). 1318-1331.
- 14 Johnson, R. P., & Buckby, R. J. Composite structures of steel and concrete. Blackwell
15 Scientific Publications. Oxford (England). (1994).
- 16 Jung, C.H., Kim, S.H., Choi, K.T., Park, S.J. & Park, S.M. Experimental shear resistance
17 evaluation of Y-type perfobond rib shear connector. *Journal of Constructional Steel*
18 *Research*, 82. (2013). 1-18.
- 19 Lawan, M., Tahir, M., Ngian, S. & Sulaiman, A. Structural performance of cold-formed
20 steel section in composite structures: A review. *Jurnal Teknologi*. 74:4. (2015) 65-
21 175.
- 22 Lawan, M. & Tahir, M. Strength capacity of bolted shear connectors with cold-formed
23 steel section integrated as composite beam in self-compacting concrete. *Jurnal*
24 *Teknologi*. 77:16. (2015) 105-112.
- 25 Lawan, M., Tahir, M., & Hosseinpour, E. Feasibility of using bolted shear connector with
26 cold-formed steel in composite construction. *Jurnal Teknologi*. 78:6-12. (2016) 7-13.
- 27 Lawan, M., Tahir, M., & Mirza, J. Bolted shear connectors performance in self-
28 compacting concrete integrated with cold-formed steel section. *Latin American*
29 *Journal of Solids and Structures*. (2016) 731-749.
- 30 Lawan, M., Tahir, M., & Osman, H. Composite construction of cold-formed steel (CFS)
31 section with high strength bolted shear connector. *Jurnal Teknologi*. 77:16. (2015)
32 171-179.
- 33 Liu, Y., Zheng, S., Yoda, T. & Lin, W. Parametric study on shear capacity of circular-hole
34 and long-hole perfobond shear connector. *Journal of Constructional Steel Research*,
35 117. (2016). 64-80.
- 36 Majdi, Y., Hsu, C., & Zarei, M. Finite element analysis of new composite floors having
37 cold-formed steel and concrete slab. *Engineering Structures*, 77. (2014). 65–83.
- 38 Majdi, Y., Hsu, C., & Zarei, M. Finite element modeling of new composite floors having
39 cold-formed steel and concrete slab. In *International Specialty Conference on Recent*
40 *Research and Developments in Cold-Formed Steel Design and Construction*, (2014).
41 463-477.
- 42 Medberry, S.B. & Shahrooz, B.M. perfobond shear connector for composite construction.
43 *Engineering Journal AISC*, 39(1). (2002). 2-12.
- 44 Oguejiofor E.C & Hosain MU. A parametric study of perfobond rib shear connectors.
45 *Canadian Journal of Civil Engineering*, 21. (1994). 614-625.
- 46 Oguejiofor E.C & Hosain MU. Numerical analysis of push-out specimenes with
47 perfobond rib connectors. *Computers & Structures*, 64 (4). (1997). 617-624.
- 48 Sara, B.M. & Bahram, M.S. perfobond shear connectors for composite consruction.
49 *Engineering Journal*, First Quarter. (2002). 2-12.

- 1 Tahir, M., Saggaff, A., Azimi, M. & Lawan, M. Impact of bolted shear connector spacing
2 in composite beam incorporating cold formed steel of channel lipped section. IIOAB
3 Journal, 7. (2016). 441-445.
- 4 Tahir, M.M., Bamaga, S.O., Tan, C.S., Shek, P.N. & Aghlara, R. Push-out test on three
5 innovative shear connectors for composite cold-formed steel concrete beams.
6 Construction and Building Materials, 223. (2019). 288-298.
- 7 Tahir, M., Bamaga, S., Ngian, S., Mohamad, S., Sulaiman, A., & Aghlara, R. Structural
8 behaviour of cold-formed steel of double C-lipped channel sections integrated with
9 concrete slabs as composite beams. Latin American Journal of Solids and Structures,
10 16(5),. (2019). 1–15.
- 11 Titoum, M., Mazoz, A., Benanane, A. & Ouinas, D. Experimental study and finite element
12 modelling of push-out test on a new shear connector of I-shape. Advanced Steel
13 Construction Vol.12, N°4. (2016). 487–506.
- 14 Verissimo, G.S. Development of a shear connector plate gear for composite structures of
15 steel and concrete and study their behavior (In Portuguese). Thesis of PhD's degree.
16 Universidad Federal de Minas Gerais Belo Horizonte. (2007).
- 17 Zhao, C. & Liu, Y.Q. Experimental study of shear capacity of perfobond connector.
18 Journal of Engineering Mechanics, 29(12). (2012). 349-354.
- 19 Shariati, M., Khorramian, K., Maleki, S., Jalali, A. & Tahir, M.M. Numerical analysis of
20 tilted angle shear connectors in steel-concrete composite systems. Steel and
21 Composite Structures, Vol.23(1). (2017). 67-85.